The performance of a Horizontal Ground Heat Exchanger (HGHE) under the seasonal ground energy storage behaviour.

Fujiao Tang[1,3], *Mojdeh* Lahoori[2], *Hossein* Nowamooz[1], *Sandrine* Rosin-Paumier[2], *and Farimah* Masrouri[2]

[1] ICUBE, UMR 7357, CNRS, INSA de Strasbourg, 24 boulevard de la Victoire, 67084 Strasbourg, France
[2] LEMTA – CNRS UMR 7563, Université de Lorraine, Vandoeuvre-lès-Nancy F-54500, France
[3] School of Transportation Science and Technology, Harbin Institute of Technology, 15900 Harbin, China

Abstract. A well-known backfill soil was considered to be used as the backfill substitutive material. The hydrothermal properties of the backfill material were estimated in laboratory and then injected in a numerical framework considering the atmosphere-soil-HGHE interaction. Numerical simulations were performed for a HGHE installed in the compacted backfill soil and the local materials. Two heat storage scenarios at three different installation depths were also investigated. The results show that an inlet fluid temperature of 50°C in summer increases highly the system performance (13.7% to 41.4%) while the improvement is less significant (0% to 4.8%) for the ambient inlet temperature scenario. A deeper installation depth increases also the system performance.

1 Introduction

Shallow geothermal energy is one of the many sources of renewable energy, and it can be easily accessed all around the world [1–3]. The temperature of the ground can be exploited during winter using a ground source heat pump for space heating and during summer for cooling needs. To increase the efficiency of shallow geothermal energy the solar energy can be stored during summer to increase the temperature of the ground [4]. Generally, open and closed heat exchangers are available for the exploitation of shallow geothermal energy [5], which are then served as low-potential sources of thermal energy for heat pumps [6, 7]. Horizontal Ground Heat Exchanger (HGHE) is one of those closed loop heat exchangers. Compared to Vertical Ground Heat Exchanger (VGHE), it is more cost effective although it requires more installation space [8].

The experimental investigations [9] showed that the thermal performance depends on the depth of HGHE installation. Due to the shallow installation depth (conventionally between 1.0 and 2.0 m) [10, 11], HGHE is also more sensitive to the meteorological condition. The results reported by Elminshawy et al. [12] showed that the thermal performance of the horizontal system highly depends on the soil compaction state (water content and density) and air flow rate. By increasing density, the solid particles are better packed into a unit volume and the number of contact points between the particles increases [13]. These contact points provide a larger heat transfer by conduction which causes the temperature variation between the inlet and outlet airflow. These observations are in agreement with the study of Hurtado et al. [14] which investigated the capacity of compacted soil to store thermal energy from the chimney power plant using an analytical model based on a finite volume procedure. They mentioned that the output power energy was increased by 10% when the soil compaction increased from loose to dense level.

Since the experimental investigations are time and money consuming, the thermal performance of horizontal heat exchanger loops in soils has been numerically investigated using finite element and finite difference tools in different studies. Normally in these models, the simulation is done by considering a homogeneous soil mass with constant thermal properties and the heat transfer is modeled by conduction using solid particles of soil [15]. However, in unsaturated compacted soils, the thermal properties will change by temperature variations, soil physical and hydraulic properties. Therefore, a comprehensive investigation is a thermo-hydraulic simulation with consideration of the mass transfer by vapor and liquid flows [16–19]. Asgari et al. [19] showed that the thermal performance of the linear and slinky types of HGHE increases by increasing the number of layers arrangement in the ground. For the spiral type exchangers, the thermal performance did not change with increasing the number of layers. Gan [16] showed that during heat extraction in winter, a deeper positioning of loops is more beneficial. At deeper position, the soil thermal properties are not affected by the daily and seasonally ambient temperature variation. Moreover, this feature has been confirmed by experimental investigation. Boukelia [20] investigated the heat lost in a seasonal storage system in an embankment using HGHE by conducting the coupled thermo-hydraulic numerical simulations with a finite element tool (Code-Bright). The author observed that when the inlet temperature in the HGHE during summer was 50 °C, the temperature of the soil close to the probes

reached 38 °C. At the end of the autumn when the thermal extraction season started, the temperature was about 25 °C, therefore, about 13 °C of heat loss has been occurred. Jradi et al. (2017) [15] showed the efficiency of the air source heat pump (ASHP) combined with a solar power system as a basis for seasonal thermal energy storage. They showed also that a huge heat loss occurred after storage seasons. Therefore, to increase the thermal performance of a medium to store thermal energy, the insulation material might be a good option and it can be taken into account in the design stage.

Another challenging issue is the consideration of the atmosphere-soil-HGHE interaction in the prediction of the system performance. Tang and Nowamooz [21] proposed a numerical simulation framework to evaluate the HGHE performance in field conditions by considering energy and water balance on the land surface. They showed in their simulations that the consideration of the atmosphere-soil-HGHE interaction underestimates highly the outlet temperature especially for the horizontal systems installed close to the soil surface up to a difference of 48%. The same effect has also been noticed by Zhou et al. [22].

The good capacity of the numerical framework considering the atmosphere-soil-HGHE interaction makes possible to bring some further responses on the backfill soil characteristics rarely studied so far. This point is very crucial for the thermal performance of the horizontal systems. Changing the surface soil may significantly improve the system performance.

In this context, this investigation aims to visualize how the soil backfill and its installation depth influence the HGHE performance. Therefore, a compacted backfill soil that its hydrothermal behavior has been experimentally investigated is considered. Then, hydrothermal properties of the compacted soil are estimated and injected in the numerical framework considering the atmosphere-soil-HGHE interaction. The thermal energy storage scenarios are also evaluated in the numerical simulations.

2 Numerical simulation model

2.1 Physic equations

The primary equations in the numerical simulation model is shown in Table 1.

Table 1. Principal equations of atmosphere-soil-HGHE interaction

Type of interaction	Principal equation
Soil surface energy balance [23]–[30]	$R_n + H - LE - G = 0$ $R_n = (1 - a_l)R_s + (R_a - \varepsilon\sigma T_s^4)$ $H = \rho_a C_{p-a}(T_a - T_s) / r_a$ $E = P \cdot \left[1 + (E_p / P)^{-2}\right]^{-\frac{1}{2}}$ $LAI = 24 \cdot h_c$ for clipped grass or $LAI = 5.5 + 1.5\ln(h_c)$ for other crops
Soil surface water balance [31]	$P = W_r + E + W_i$
Richard equation for hydraulic transfer is soil	$\rho_w \cdot \psi \cdot \frac{\partial H_p}{\partial t} + \nabla \cdot \left[-K \cdot k_r \cdot \nabla \cdot \rho_w \cdot \left(H_p + D + H_k\right)\right] = 0$
Hydrothermal transfer in subsurface soil	$\rho_s C_{p-s} \frac{\partial T_s}{\partial t} + \nabla \cdot \left(\rho_w C_{p-w} u_w T_s\right) = \nabla \cdot (k_s \nabla T_s) + Q_s$
Heat transfer in pipe	$A\rho_f C_{p-f} \frac{\partial T_f}{\partial t} + A\rho_f C_{p-f} u_f \cdot \nabla T_f = \nabla \cdot A k_f \nabla T_f + f_D \frac{\rho_f A}{2 d_h} \lvert u_f \rvert u_f^2 + Q$ $Q_{wall} = h_{\text{int}} \cdot Z \cdot (T_{i-p} - T_f)$

R_n is the net radiation heat flux (W.m^{-2}), H is the sensible heat flux (W.m^{-2}), LE is the latent heat flux (W.m^{-2}), G is the ground heat flux (Wm^{-2}), a_l is the surface albedo, R_s is the shortwave radiation (W.m^{-2}), R_a is the incoming longwave radiation (W.m^{-2}), $\varepsilon\sigma T_s^4$ is the outcoming longwave radiation (W.m^{-2}), ε is the soil surface emissivity, σ is Stephan-Boltzman constant (Wm^{-2}K^{-4}), T_s and T_a are the soil and the ambiant temperatures (K), ρ_a is the air density (kgm^{-3}), C_{p-a} is the air specific heat capacity (Jkg^{-1}K^{-1}), r_a is the aerodynamic resistance to heat transfer (sm^{-1}), P is the rainfall rate (mms^{-1}), E_p is the evaporation potential (kgm^{-2}s^{-1} or mms^{-1}), LAI is the leaf area index, h_c is the displacement height is linear to the vegetation height (m), water run off (W_r), actual evaporation (E), and infiltration (W_i), where ρ_w is the water density (kgm^{-3}), ψ is the specific moisture capacity (m^{-1}), H_p is the suction head (m), t is the time (s), K is the hydraulic conductivity (ms^{-1}), k_r is the relative hydraulic conductivity, D is the elevation head (m), H_k is the kinetic head (m), ρ_s is the soil density (kgm^{-3}), C_{p-s} is the soil heat capacity (Jkg^{-1}K^{-1}), T_s is the soil temperature (°C), C_{p-w} is the water specific heat capacity (Jkg^{-1}K^{-1}), u_w is the water velocity in soil (ms^{-1}), Q_s is the soil heat source (Wm^{-3}), A is the pipe inner cross-sectional area (m^2), ρ_f is the fluid density (kgm^{-3}), C_{p-f} is the fluid specific heat capacity (Jkg^{-1}K^{-1}), T_f is the fluid temperature (°C), u_f is the fluid flowing velocity (ms^{-1}), k_f is the fluid thermal conductivity (Wm^{-1}K^{-1}), f_D is the Darcy friction factor, d_h is the hydraulic diameter (m) and Q_{wall} is the energy from the surrounding media (Wm^{-1}), h_{int} is the film heat transfer coefficient (Wm^{-2}K^{-1}). Z is the pipe inner perimeter (m) and T_{i-p} is the inner pipe temperature (°C).

2.2 Geotechnical condition

We considered that the HGHE system is installed in Alsace region in France in June. The local soil till 1 m of depth (installation depth) around the HGHE is completely replaced by the backfill soil.

The backfill soil is frequently used in France [32]. The material was classified as sandy lean clay, CL, according to the Unified Soil Classification System [33]. Regarding the X-ray diffractograms analysis the

compacted soil contains 81% quartz, 7% dolomite, 5% calcite, 5% clayey materials and 3% feldspar. According to the particle-size distribution, almost 20% of the particles of the soil were smaller than 2 µm corresponding to the clay content, and 59 % were higher than 0.05 mm corresponding to the sand content (xs). With a liquid limit (LL) of 27% and a plastic limit (PL) of 21%, the plasticity index (PI) was 6%. The backfill soil is compacted at a water content of 16.3% to reach a dry density of 1.72 Mg.m^{-3} as a reference state.

Fig. 1 shows the variation of the water content with the suction for the compacted soil at its reference state.

Fig. 2 shows the variation of the hydraulic conductivity of the studied material with suction. The hydraulic conductivity was measured in saturated conditions with triaxial device and in the unsaturated state with the Wind method [34].

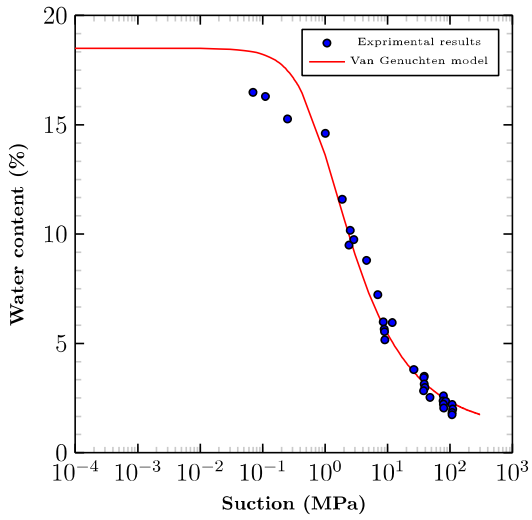

Fig. 1. SWRC of the studied backfill soil at the reference compaction state (dry density = 1.72 Mg.m^{-3}).

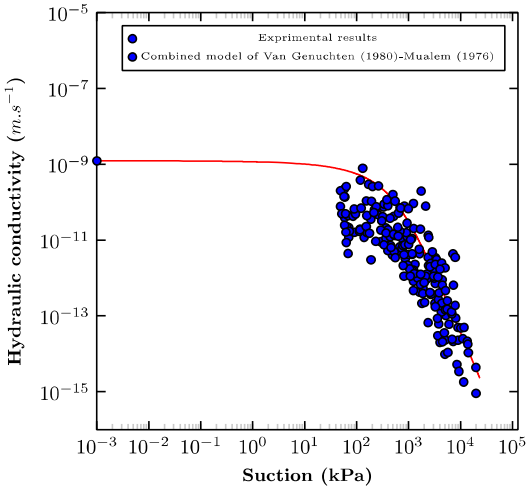

Fig. 2. Hydraulic conductivity of the studied backfill soil.

2.3 Model geometry

The studied geometry has a length of 30 m, a width of 12 m and a height of 20 m (Fig. 3). This deep geometry was selected to have no hydrothermal impact of the seasonal metrological condition on the bottom boundary. A slinky-type HGHE with 0.03 m of inner diameter and 0.036 m of outer diameter is installed 1 m below surface, covered with the backfill soil compacted at dry densities of 1.72 Mg.m^{-3}.

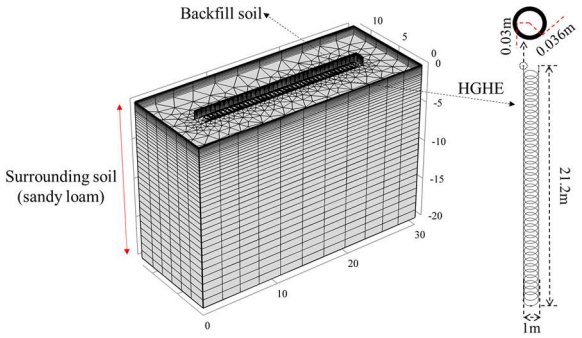

Fig. 3. Geometry and its mesh for the numerical simulations.

2.4 Boundary and meteorological condition

The temperature gradient at the bottom boundary is set 0.142 K.m^{-1} [35], and the extra water from the precipitation is drained at the bottom boundary. The groundwater level is set constant at the depth of 7.5 m in the whole year. No hydrothermal flow is imposed on the lateral boundaries.

The meteorological condition corresponds to the local condition [36] with the installation time in June. Fig. 4a and Fig. 4b present the ambient temperatures and the shortwave radiation for one year represented by a simplified sinusoidal curve.

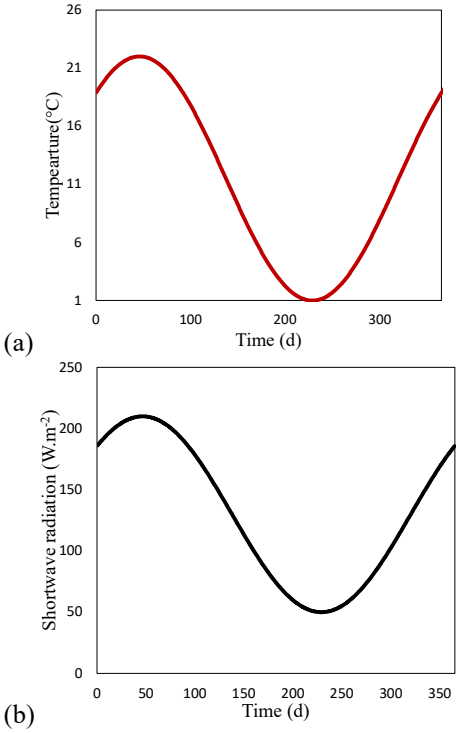

Fig. 4. Simplified local meteorological condition:
(a) Ambient temperature fluctuation for one year and
(b) shortwave radiation fluctuation for one year.

At the site, there is no obvious seasonal fluctuation of cloud cover, wind speed, precipitation and air humidity

with time. Therefore, an average cloud cover of 0.41, an average wind speed of 2 $m.s^{-1}$, an average monthly precipitation of 55.7 mm, and an average air humidity of 83% are applied in the numerical simulation model to capture the main meteorological condition of the local site.

For the surface water balance, 20% of precipitation run off, and the other 80% participate into evapotranspiration or infiltration.

2.5 Initial hydrothermal conditions

An equilibrium method (proposed by Tang & Nowamooz [36]) is used to obtain the initial hydrothermal profiles at its installation time in the end of summer.

2.6 Pipe and its carrying fluid

The pipe is a High-Density Polyethylene Pipe (HDPE) with the thermal conductivity of 0.4 W.m-1.K^{-1}. Propylene Glycol (PG) with a volume concentration of 25% is selected as the carrying fluid. It has a dynamic viscosity of 0.0055 Pa.s, a density of 1026 kg.m-3, a thermal conductivity of 0.45 $W.m^{-1}.K^{-1}$ and a specific heat capacity of 3974 $J.kg^{-1}.K^{-1}$ [37]. The carrying fluid velocity is 0.5 $m.s^{-1}$ during the operation period.

3 Heat storage effect on the performance of HGHE installed in backfill soil

In this section, the effect of thermal energy storage during summer on the HGHE performance installed in compacted backfill soil is investigated. The results are compared to the original system with no heat storage (called Nsto scenario in this section). Several installation depths are also tested in the numerical simulations.

3.1 Studied scenarios and installation depths

The context of thermal energy storage is increasing the performance of the HGHE by increasing the temperature of ground. Therefore, during summer, a fluid with higher temperature than the ground can circulate through the HGHE to exchange the temperature with surrounding soil. The stored heat is expected to be released during winter. The stored energy during summer season is extracted by a circulating fluid with a temperature of 1°C in the HGHE during winter. The system stops working at the end of Winter.

To store thermal energy in soil during summer season and use it in winter, two different scenarios are investigated in this study (Table 2).

3.1.1 First scenario (StoA)

A reservoir of carrying fluid is exposed to exterior temperature and then the carrying fluid circulates in HGHE during summer. Therefore, the inlet temperature in 3 months of summer is the ambient temperature (scenario StoA) as presented in Fig. 4 (temperatures of 0 to 92 days). This system is in relaxation in Autumn (from 92nd to 183rd day), therefore no fluid flow will be circulated through the system. When Winter comes (from 183rd to 274th day), a fluid flow with inlet temperature of 1°C will be circulated. Again the system is in relaxation in Spring (from 274rd to 365th day) (Table 2).

Table 2. Imposed temperature of inlet fluid for StoA and Sto50.

Season	Scenario	
	StoA	Sto50
Summer Day 0 to 92	Ambient temperature (Fig. 4)	50 °C
Autumn Day 92 to 183	relaxation	relaxation
Winter Day 183 to 274	1 °C	1 °C
Spring Day 274 to 365	relaxation	relaxation

3.1.2 Second scenario (Sto50)

Solar panels absorb the solar energy and the energy can be used to heat the subsurface soil in summer while a fluid with a constant inlet temperature is circulating in the HGHE. Therefore, the inlet temperature in 3 months of summer is a constant temperature of 50 °C (Sto50) as presented in Fig. 5. The system works the same way as the ambient temperature storage scenario except that the inlet temperature is 50 °C in Summer season (Table 2). Due to the interaction with ground surface, the stored energy during relaxation seasons is dissipated into the atmosphere. If the HGHE is installed close to the land surface, a higher amount of stored energy can be dissipated. Therefore, three depths of at 1, 1.5 and 2 m beneath land surface are investigated for both scenarios to study the influence of installation depth on the HGHE performance.

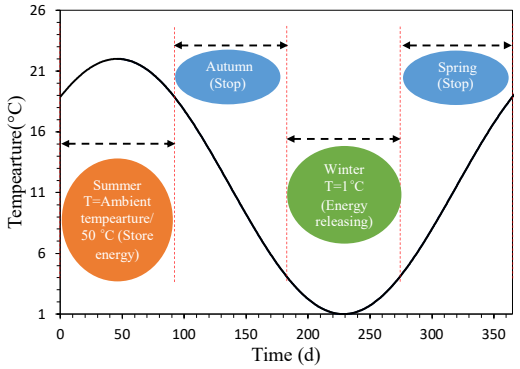

Fig. 5. Operation mode for the HGHE over one year.

3.2 Simulation results

3.2.1 Scenario 1 (StoA) compared to scenario with no heat storage (Nsto).

Fig. 6 shows the pipe outlet temperature with time at the installation depths of 1, 1.5 and 2 m for the first scenario

(StoA) compared to the outlet temperatures of the original HGHE with no heat storage (Nsto) presented in section 4. The figure shows the fluid outlet temperature decreases abruptly with the working of the HGHE. Afterwards, the fluid temperature generally decreases and starts to increase with warmer climate. In addition, the figure shows that outlet temperature increases by depth.

3.2.2 Scenario 2 (Sto50) compared to scenario with no heat storage (Nsto).

Fig. 7 shows the outlet temperature for the second storage scenario (Sto50) at three installation depths compared to the outlet temperatures of the original HGHE with no heat storage (Nsto) presented in section 4. The figure shows that the ground temperature is obviously improved in summer, and the deeper the installation depth, the larger difference between the outlet temperatures of the scenario considering and non-considering the energy storage in summer.

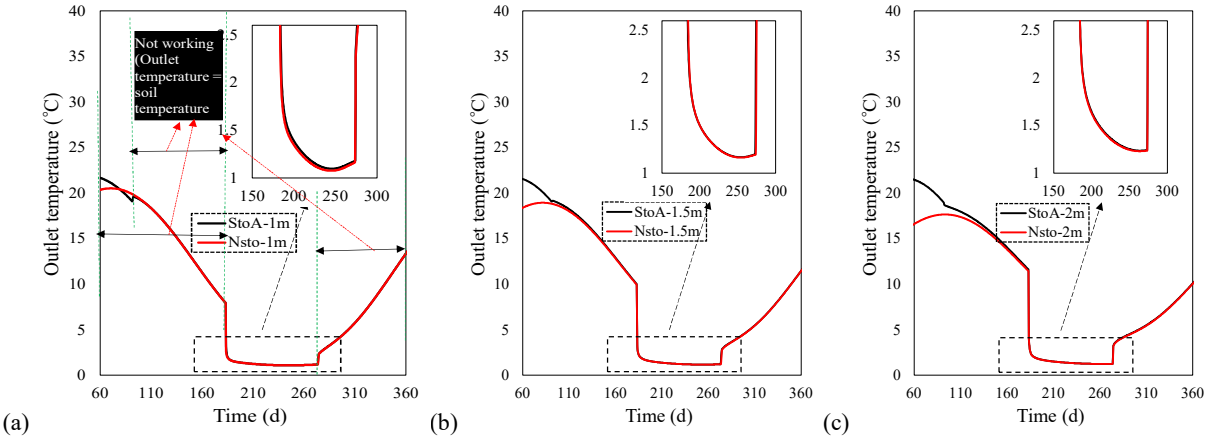

Fig. 6 Outlet temperature comparison of the storage scenario (ambient temperature) and the non-storage scenario for three installation depths a) 1m, b) 1.5m and c) 2

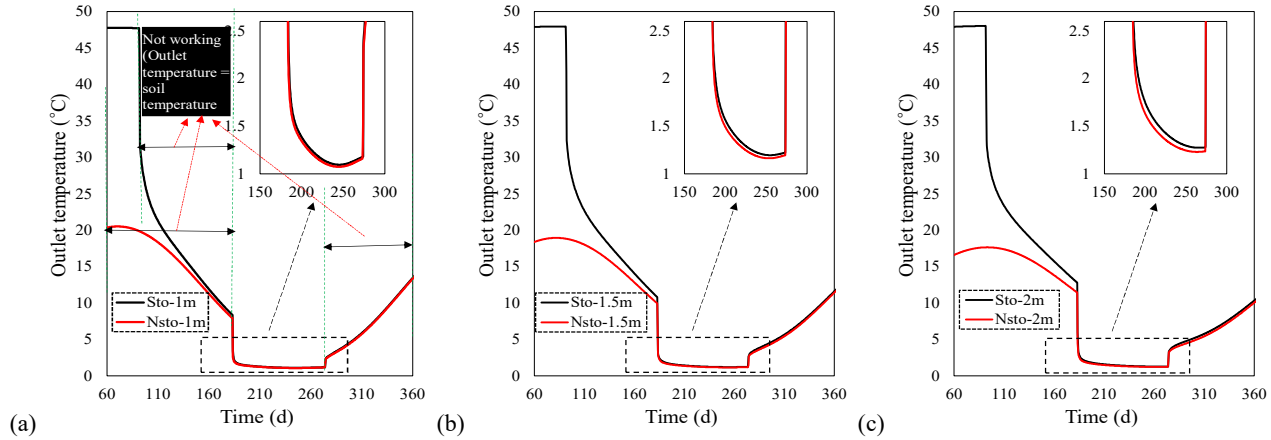

Fig. 7 Outlet temperature comparison of the storage scenario (50 °C of inlet temperature during summer) and the non-storage scenario for three installation depths a) 1m, b) 1.5m and c) 2m.

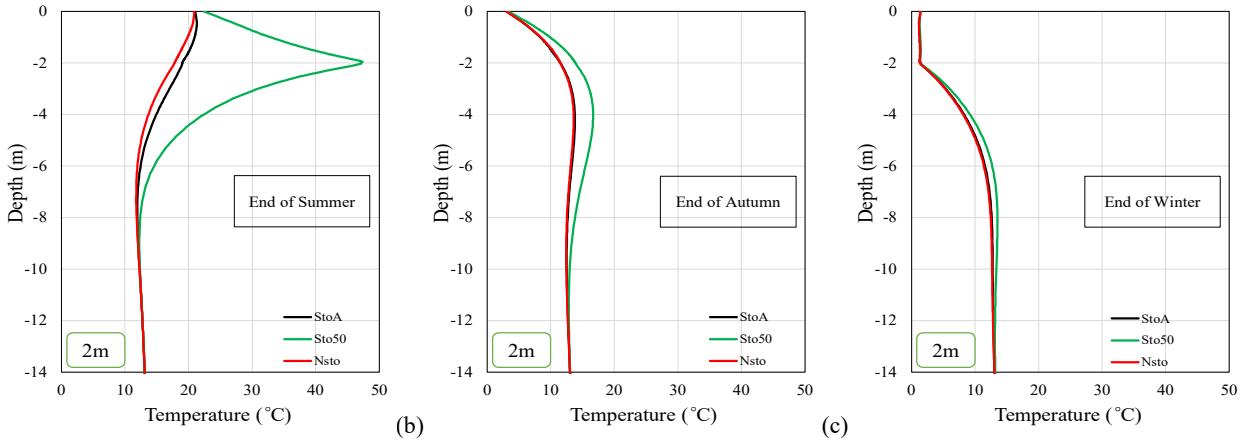

Fig. 8 Temperature profiles at the end of Summer (a), Autumn (b) and Winter (c)

4 Comparison of different studied scenarios

The surrounding temperatures of the HGHE installed at the depth of 2 m in the end of Summer, Autumn and Winter are shown in Fig. 8. The figure shows that the soil temperature has been clearly improved in the scenario with 50 °C of fluid inlet temperature in Summer (Sto50), while the surrounding temperature improves negligibly with the atmosphere temperature storage scenario (StoA). Specifically, soil temperature has been improved 27 °C and 3 °C respectively at the depth of 2 m at the end of Summer and Autumn with the energy storage scenario (Sto50).

Fig. 9 compares the annual TEE values of the aforementioned heat storage scenarios (StoA and Sto50) with the TEE values of the original scenario without heat storage (Nsto). The figure shows that the HGHE can be highly improved by adopting an inlet fluid temperature of 50°C in summer while the ambient inlet temperature produces less amelioration in the HGHE performance.

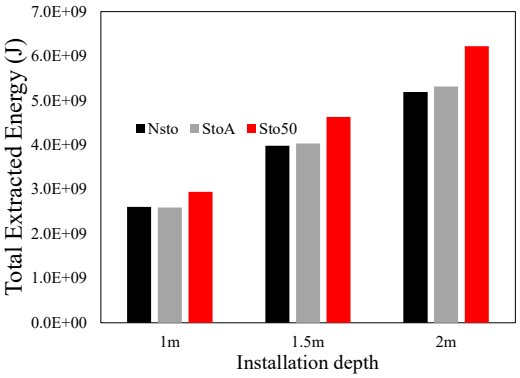

Fig. 9 Comparison between the heat storage scenarios (StoA & Sto50) with non-storage scenario (Nsto) at three different installation depths

5 Conclusion

A well-known backfill soil was used to improve the performance of an HGHE system installed in the east of France. The hydrothermal properties of the backfill soil were first injected in a numerical framework considering the atmosphere-soil-HGHE interaction.

To improve the HGHE performance, two heat storage scenarios at three different installation depths were studied. The results show that an inlet fluid temperature of 50°C in summer increases highly the system performance (13.7 to 41.4%) while the improvement is less significant (0 to 4.8%) for the ambient inlet temperature. A deeper installation depth increases the total extracted energy (TEE) but increases the installation costs.

References

1. R. Shortall, B. Davidsdottir, G. Axelsson, Renew. Sustain. Energy Rev. **44**, 391 (2015)
2. R. Sangi, D. Müller, J. Build. Eng. **16**, 159 (2018)
3. A. H. Abedin, Open Renew. Energy J. **4**, 42 (2011)
4. J. Xu, R. Z. Wang, Y. Li, Sol. Energy **103**, 610 (2014)
5. G. Florides, S. Kalogirou, Renew. Energy 32, 2461 (2007)
6. Y. Yuan, X. Cao, L. Sun, B. Lei, N. Yu, Renew. Sustain. Energy Rev. **16**, 6814 (2012)
7. D. Adamovsky, P. Neuberger, R. Adamovsky, Energy Build. **92**, 107 (2015)
8. S. J. Self, B. V. Reddy, M. A. Rosen, Appl. Energy **101**, 341 (2013)
9. R. A. Beier, W. A. Holloway, Appl. Therm. Eng. **78**, 1 (2015)
10. R. Garcia Gonzalez, A. Verhoef, P. L. Vidale, B. Main, G. Gan, Y. Wu, Renew. Energy **44**, 141 (2012)
11. M. Habibi, A. Hakkaki-Fard, Energy Convers. Manag. **171**, 1177 (2018)
12. N. A. S. Elminshawy, F. R. Siddiqui, Q. U. Farooq, M. F. Addas, Appl. Therm. Eng. **124**, 1319 (2017)
13. N. H. Abu-Hamdeh, R. C. Reeder, Soil Sci Soc Am J **64**, 6 (2000)
14. F. J. Hurtado, A. S. Kaiser, B. Zamora, Energy **47**, 213 (2012)
15. M. Jradi, C. Veje, B. N. Jørgensen, Appl. Therm. Eng. **114**, 360 (2017)
16. G. Gan, Int. J. Low-Carbon Technol. **8**, 95 (2013)
17. Y. Gao et al., Energy Build. **110**, 302 (2016)
18. C. Li, P. J. Cleall, J. Mao, J. J. Muñoz-Criollo, Appl. Therm. Eng. **139**, 307 (2018)
19. B. Asgari, M. Habibi, A. Hakkaki-Fard, Appl. Therm. Eng. **167**, 114770 (2020)
20. A. Boukelia, PhD Thesis, Université de Lorraine, France, 2016.
21. F. Tang H. Nowamooz, Renew. Energy **146**, 705 (2020)
22. K. Zhou, J. Mao, Y. Li, Z. Hua, Energy Convers. Manag. **225**, 113469 (2020)
23. M. Chalhoub, M. Bernier, Y. Coquet, M. Philippe, Renew. Energy **103**, 295 (2017)
24. R. G. Allen, J. Irrig. Drain. Eng. **112**, 348 (1986)
25. L. Turc, Ann. Agron. **5**, 491 (1954).
26. J. G. Pike, J. Hydrol. **2**, 116 (1964)
27. X. Chen, S. G. Buchberger, Hydrol. Earth Syst. Sci. **22**, 4535 (2018)
28. A. M. J. Gerrits, H. H. G. Savenije, E. J. M. Veling, L. Pfister, Water Resour. Res. **45**, (2009)
29. J. Monteith, Symp. Soc. Exp. Biol. **19**, 205 (1965)
30. R. G. Allen, M. E. Jensen, J. L. Wright, R. D. Burman, Agron. J. **81**, 650 (1989)
31. O. Dietrich, M. Fahle, M. Seyfarth, Agric. Water Manag. **163**, 75 (2016)
32. M. Lahoori, Y. Jannot, S. Rosin, A. Boukelia, F. Masrouri, Appl. Therm. Eng. **167**, 114795, (2020)
33. ASTM Standard D2487, ASTM Int. Conshohocken PA, 2000.
34. G. P. Wind, *Capillary conductivity data estimated by a simple method (No. 80),* 1966.
35. P. Baillieux, E. Schill, J.-B. Edel, G. Mauri, Int. Geol. Rev. **55**, 1744 (2013)
36. F. Tang, H. Nowamooz, Renew. Energy **128**, 210 (2018)